https://doi.org/10.1016/j.nanoen.2021.105867

Organogel Electrode Based Continuous Fiber with Large-scale Production for Stretchable Triboelectric Nanogenerator Textiles

Titao Jing, Bingang Xu,* Yujue Yang

Nanotechnology Center, Institute of Textiles and Clothing, The Hong Kong

Polytechnic University, Hung Hom, Kowloon 999077, Hong Kong

* Corresponding author, E-mail: tcxubg@polyu.edu.hk

Abstract:

Wearable electronics had drawn great attentions in recent years because of their valuable applications in our daily lives. Among them, triboelectric nanogenerator (TENG) textile was a promising candidate to alleviate electricity supply problem of wearable electronics. However, currently used electrodes in TENG textile are hard to fulfill the requirements of stretchable electronics. Here, organogel conductor was proposed as electrode to construct triboelectric fiber (GS-fiber), owing to its merits of flexibility, stretchability and conductivity. The core/shell structure GS-fiber was prepared from gel's photo-crosslinking in transparent silicone hollow fiber, in which hollow fiber was the mold for gel electrode and outer friction layer. The flexibility and solid form of organogel electrode avoided the cracking problem of metallic electrode and leakage problem of liquid electrode in TENG textile, which make GS-fiber a stretchable and tailorable fiber. Moreover, the facile preparation process endowed GS-fiber with large-scale production ability and 30-meter GS-fiber was prepared for demonstration. The GS-fiber was then knitted into TENG textile (GS-teng) for bio-mechanical energy harvesting. This work indicated that organogel electrode has great potential in triboelectric fiber, which was a remarkable progress towards TENG textiles' industrial application.

Key words: Wearable electronics; Organogel electrode fiber; Textile based triboelectric nanogenerator; Large-scale production; Knitting

1. Introduction

Next-generation wearable and portable electronics have drawn great attentions in recent decades because of their promising potentials in health monitoring devices, artificial electronic skins and tactile sensors, etc.[1-8] However, the electricity supply of such wearable electronics has been more and more in demand and the traditional batteries are overwhelmed due to the limited capacity of electricity and lifetime, heavy package as well as inflexible framework.[6-10] To address the issue, researchers put immense enthusiasm in wearable generators which could intimately integrate with the human body and transfer ambient energy to electricity.[11-13] Among various generators, triboelectric nanogenerator (TENG), which was invented in 2012 by Zhonglin Wang, has exhibited promising potentials owing to the nature merits of vast material choices, simple structure, high body integration and energy conversion efficiency.[14-21] The structure of TENG was usually consisted of two friction materials with distinct electron affinities and corresponding back electrodes for charge collection, in which the friction materials' contact and separation would result in tribo-electrification and subsequent electrostatic induction in back electrodes. Among various types of TENG, textile based TENG was outstanding and had been regarded as a promising wearable generators in past years because of textile's nature advantages such as comfortability, versatility and high integration with human body.[10, 15, 22]

Nonetheless, many challenges lie on the way to TENG textile, which hinder the advent of wearable electronics.[19, 23, 24] One of the most difficult issue is the electrode in TENG textile as the well assembling of friction dielectric yarn or fiber and electrode in a long and thin continuous fiber was a great challenge.[22] Besides, the

characteristics of textile required that the triboelectric fiber are tailorable and stretchable for textile fabrication and comfort in human body. To date, several types of electrode from metallic wire, conductive fabric or fiber to liquid conductor have been employed in TENG textile for the purposes of flexible and comfortable energy harvesting textile with high output performance.[24] However, metallic wire such as stainless wire faces the cracking problem when the TENG textile is suffered enfoldment in daily life.[9] The stretchability of metallic wire also limits its applications in stretchable TENGs.[17, 25] Some researchers proposed liquid metal or ionic solutions electrode because of liquid's advantage of deformability, which could avoid the cracking problem.[26-28] Unfortunately, when the textile was tailored or damaged, the leakage of whole liquid conductor was emerged, which further resulted in invalidation of whole TENG textile. Another difficult issue is the large-scale production of TENG textiles or fibers with stretchability.[17, 25] Some works proposed special structures such as helix fiber for stretchability.[17, 29] Nonetheless, the complex structure induced large size of fiber, which further resulted in weight problem of the corresponding textiles. Conductive fabric or fiber, featured with flexibility and solid state, is an promising candidate electrode in TENG textile. However, the currently used conductive fabrics or fibers are usually prepared from uniform dispersion of conductive materials such as Ag nanowire, carbon nanotube on fabric or fiber, which are hard to be scaled-up because of complex fabrication process.[3, 29-32] These drawbacks of currently used electrodes hinder the development of TENG textile. Flexible and stretchable

electrodes which are suitable for TENG textile are thereby in an urgent demand and will significantly promote the advent of wearable power generator.

Gel electrode is composed of 3D polymer-chain frame and swelling ionic solvent, which is facilely synthetized from crosslinking-polymerization of monomer and swelling solvent mixed liquid.[33-38] The gel electrode is naturally endowed with advantages of softness, flexibility and conductivity in solid form, which was excellent candidate of electrode for flexible TENG and had been proven its value in some recent works.[34, 39-45] Furthermore, the liquid-solid form state transform of gel fabrication is suitable to prepare different shapes electrode via designed mold. Accordingly, the gel electrode could be fabricated in fiber shape which should have the potential in TENG textile to address the aforementioned challenges as the gel's flexible and conductive solid form as well as facile preparation process.[44, 46-48] In addition, organogel electrode was supposed to be more durable than hydrogel in fiber due to the large temperature range between freezing and boiling point of organic swollen solvent.

Herein, we employed organogel electrode to construct fiber and textile based TENGs for the demonstration of the concept of organogel electrode based continuous triboelectric fiber (GS-fiber) in large-scale production based on our previous work about organogel electrode.[45] The gel electrode was prepared from photo-crosslinking of 4-acryloylmorpholine (ACMO) monomer and propylene carbonate solvent mixed pre-cured liquid in a transparent thin silicone hollow fiber and the organic swollen solvent of organogel endowed GS-fiber with large working temperature range to resist solvent evaporation.[45] The silicone hollow fiber was not only the mold for the

preparation of gel electrode fiber but also the outer friction layer of GS-fiber. The triboelectric fiber was in a gel electrode/silicone core/shell structure, in which shell silicone layer was the friction materials and gel was the back electrode. As the flowability of liquid, the pre-cured liquid of organogel electrode was easily transferred into the silicone hollow fiber with a syringe in designed length, which meant that the triboelectric fiber could be fabricated in large-scale production and a continues sample of as long as 30 meter was prepared for demonstration. Moreover, the prepared GS-fiber could be tailored into designed length for knitting, avoiding the leakage in liquid electrode based triboelectric fiber. Subsequently, a piece of 5×5 cm^2 TENG textile (GS-teng) was prepared from knitting of tailored GS-fiber, which exhibited excellent robustness in different environment owing to properties of GS-fiber. The TENG textile was an excellent power source to harvest bio-mechanical energy with an instantaneous power density of 40 mW/m^2, which was sufficient to drive LEDs and electric watch. In addition, The TENG textile could be applied as a sensor to detect human movement. This work demonstrated the gel electrode fiber's application in TENG textile because of the gel's merits of softness, flexibility, conductivity and large-scale production, which showed promising potentials to address the challenges in TENG textile and make a remarkable progress towards the target of industry application in textile based TENG.

2. Results and discussion

2.1 Organogel electrode based GS-fiber's structure and GS-teng's output performance

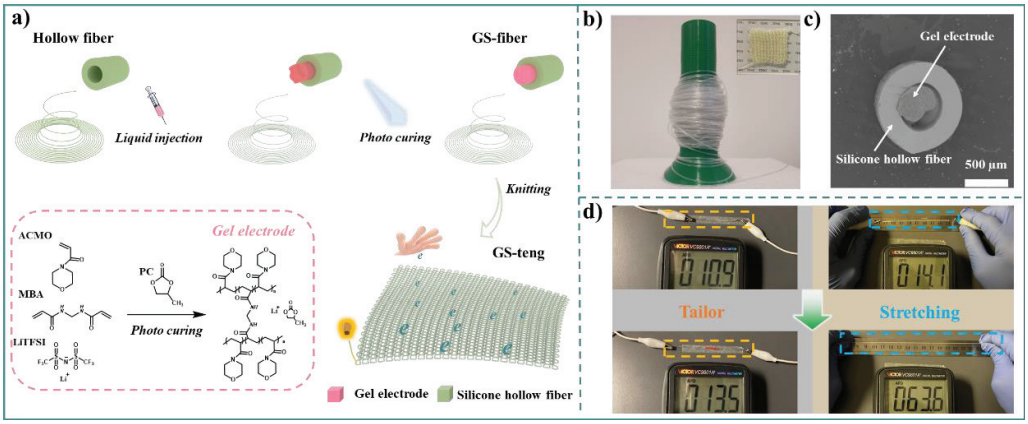

Figure 1. a) Scheme and fabrication procedure of the gel electrode based GS-fiber and TENG textile (GS-teng). b) The sample of GS-fiber with a length of 30 meters and the inset image was GS-teng with 5×5 cm^2. c) Cross-section of GS-fiber. d) The tailorable and stretchable states of GS-fiber.

The organogel electrode based GS-fiber's fabrication and gel electrode/silicone core/shell structure were schematically presented in Fig 1. The key to GS-fiber's fabrication was the fiber shape of gel electrode, which was the photo-crosslinking of pre-cured gel solution in commercial silicone hollow fiber of 1 mm outer diameter and 0.5 mm inner diameter. The pre-cured gel solution could be conveniently transferred into the thin silicone hollow fiber through syringe pumping and the facilely preparation thus endowed GS-fiber with the large-scale production ability. Under ultraviolet light irradiation, the 4-acryloylmorpholine (ACMO) monomer in pre-cured gel solution was initiated to polymerization, and the poly-ACMO 3D frame work of gel electrode was consequently formed, which was swollen by PC's LiTFSI solution conductor. The FTIR spectrum confirmed the formation of gel electrode. As shown in Fig S1, the broad spectrum of 3,500 cm^{-1} was assigned N-H from the cross-linker. The spectrum at 1,783 cm^{-1} and 1,635 cm^{-1} were the characteristic vibration bands of tertiary amide -C=O and carbonate -C=O respectively. In terms of LiTFSI, the characteristic -S=O was assigned to the spectrum of 1,353 cm^{-1}. Furthermore, the resistivity of organogel electrode was

measured as 1.83 KΩ·cm at unstretched state, indicating the organogel electrode was a good conductor for TENG electrode. Moreover, as the 3D frame work of organogel electrode, the organogel electrode could be stretched to over 450% of its initial length, demonstrating a stretchable and flexible electrode, as shown in Fig S2 and Fig S3. Meanwhile, the resistivity of organogel electrode in stretched state showed a stepwise growth, which reached to 2.75 KΩ·cm at 4-fold of its initial length.

The sample of GS-fiber with 30 meter in length was prepared for the demonstration of large-scale production potential, which was shown in Fig 1b. The formed inner solid gel electrode along with outer silicone friction layer constructed the GS-fiber with a core/shell structure which was further confirmed by the SEM results in Fig 1c. The GS-fiber's electrode and friction layer were all in solid form and could be facilely tailored in designed size with its initial core/shell structure for adaptation to different sizes' textile. As shown in Fig 1d, a piece of fiber was connected to a universal meter in circuit for demonstration of the property. The resistance value in display of universal meter was employed as indication of inner core gel's conductivity. After the fiber was tailored into two pieces of fiber, the all solid state of outer and inner layer avoided leakage problem in liquid electrode based fiber and the gel electrode/silicone core/shell structure was also kept. A metal wire was then applied to connect the two pieces of fiber's inner core gel electrode and the resistance value from universal meter proved the conductivity of whole circuit, which meant the GS-fiber was tailorable and the core/shell structure of electrode was kept. In addition, the conductivity of GS-fiber's inner electrode core in stretching state was exhibited in a similar circuit. As shown in

Fig 1d, the GS-fiber's inner electrode core still maintained its conductivity even it was stretched to over 200% of its initial length and the core/shell structure of GS-fiber was still maintained. The uniaxial tensile tests of GS-fiber and silicone hollow fiber were exhibited in Fig S4. The silicone hollow fiber was highly stretchable, reached over 700% stretchability. The Young's modulus reached 8.3 Mpa, which was much higher than organogel's 0.03Mpa. GS-fiber was a coaxial fiber that was composed of core organogel electrode and outer silicone fiber. The organogel was much softer as compared to silicone hollow fiber, which had negligible influence on GS-fiber's mechanical property. Hence, GS-fiber's stress-strain curve was similar with silicone hollow fiber's. However, when the stretchability was over 450%, the inner core of organogel electrode reached its limitation. The inner core electrode thus could be broken, which induced invalidation of GS-fiber. The operated stretchability of GS-fiber should be below the limitation of organogel around 450%. In general, the results illustrated that GS-fiber was tailorable and stretchable fiber, which could be facilely processed without the concerns of structure damage and further invalidation in liquid or metallic electrode based TENG textile. In textile preparation, tailoring and stretching were necessary procedures and the process facility thereby endowed the GS-fiber with the promising potentials in real application.

The GS-fiber was subsequently tailored into 3 m long to prepare TENG textile of 5×5 cm^2 area via hand knitting for energy harvesting device, as presented in the inset of Fig 1b. The TENG textile (GS-teng) was breathable, stretchable and soft which could intimately integrate with the human body in a comfortable way. The working model of

GS-teng was single-electrode mode and a typical working cycle was exhibited in Fig 2a. In detail, when GS-teng was brought into contact with the electron positive materials, the triboelectric outer layer of silicone in GS-teng obtained the electrons from the paired materials because the higher electron affinity of silicone. Consequently, the same amount charges with different polarities were established on the surfaces of the two paired friction materials. Once the paired materials were separated from GS-teng, the net negative charges on outer layer of silicone would result in the movement of Li^+ positive ions in gel electrode and subsequent accumulation of positive charges in inner gel electrode's interface region which were close to the outer layer of silicone. Correspondingly, the redundant negative charges of gel electrode would impel the electrons in metal wire to the ground for electrostatic equilibrium. The electric signal was thus generated due to the movement of electrons in metal wire. When the paired materials were far enough away from GS-teng, the electrostatic equilibrium state in all interface area would be reached. Once the paired materials approached to GS-teng again, the whole charges motion in gel electrode and metal wire would be in an inversional way for electrostatic equilibrium. The reversed injection of electrons from ground to metal wire thus induced reversed current and alternative current would emerge in a connected circuit if the contact-separation process of the paired materials was periodical repeated.

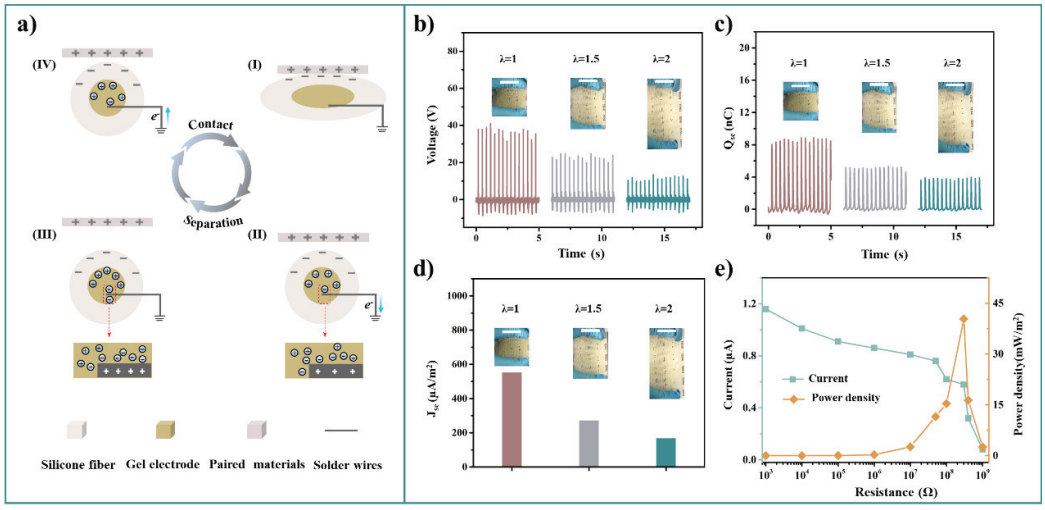

Figure 2. a) Working mechanism of GS-teng. b) Output voltages, c) short-circuit charge transfers (Q_{sc}) and d) short-circuit current densities (J_{sc}) of GS-teng at different stretched states. λ: ratio of stretched GS-teng length *versus* initial length. The scale bar is 3 cm. e) The instantaneous power density and output current of GS-teng *versus* external resistance of different values.

In order to precisely evaluate the output performance of TENG textile, the GS-teng was applied by a periodical force at frequency of 3 Hz and the paired friction material was nitrile glove of 6×6 cm^2 which was slightly larger than the size of GS-teng for fully contact. The condition was also applicable to all the tests in following paragraph for uniform comparison if there was no otherwise specification. When the nitrile glove was brought into contact and separation with GS-teng, an output amplitude could be observed, indicating the mechanical energy was successfully transferred into electric energy. As shown in Fig 2, after 1,000 times of contact-separation cycles, the output voltage achieved around 40 V and corresponding short-circuit current density (J_{sc}) also reached to 550 μA/m^2. The short-circuit charge transfer (Q_{sc}) was around 9 nC. More contact-separations were conducted for the exhibition of GS-teng's stability and no obvious change was observed in such test, as shown in Fig S5. The output performances of GS-teng at other applied forces were recorded in Fig S6. The output

performance was enhanced when the applied force was increased. Under 25 N and 100 N applied forces, the output voltage was 26 V and 57 V respectively. The Q_{sc} and J_{sc} exhibited a similar tendency when the applied force was changed. The frequency's influence on output performance was revealed by Fig S6d-f, in which 1 Hz and 2 Hz external forces were applied. The output voltage and J_{sc} were increased with the frequency while the Q_{sc} was relatively steady. The steady Q_{sc} was accounted for the same contact condition when the magnitude of force was same even when the frequency was different. In addition, GS-teng could work at stretched state, indicating it was a reliable energy harvester to adapt to the textile stretching in human body. However, the effective contact area of GS-teng was decreased due to loose packing fiber in stretched state and the output performance was subsequently weaken when GS-teng was stretched to 2-fold of its initial lengths. Furthermore, a series of external resistances with different values (10^3~10^9 Ω) were employed to demonstrate the GS-teng's ability as a power source, which were connected in series circuit. As shown in Fig 2e, the current in the series circuit dropped gradually when the external resistance was enhanced to 10^9 Ω. The instantaneous power density of GS-teng was thereby obtained from the resistance value and corresponding current which accorded to equation of $W=I^2R$. The peak instantaneous power density was 40 mW/m^2 when the external resistance of 3×10^8 Ω was connected in the circuit. The power density of GS-teng was sufficient to power many electronics, exhibiting promising potentials in wearable power sources. Moreover, other fiber based TENGs were compared with this work to further demonstrate the advantages of GS-teng, as shown in Table S1.

2.2 The robustness of GS-teng in different environments as a power generating textile

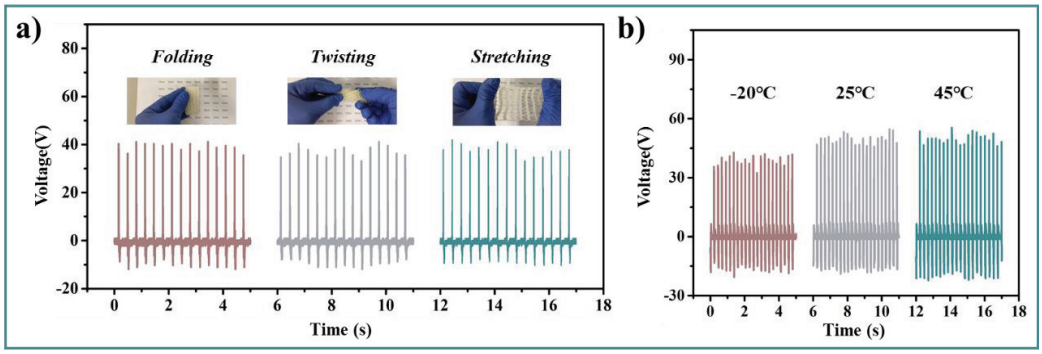

Figure 3. a) Output voltages of GS-teng after 100 cyclic times of folding, twisting and stretching respectively. b) Output voltages of GS-teng at different working temperatures, which were obtained from hand tapping.

Textiles are high integrated to human body, which will suffer different deformations in daily life. The TENG textile should be featured with steady output performance even when it was deformed by external force. Some typical deformations were thus performed on the as-prepared GS-teng to exhibit the steady output performance. As shown in Fig 3a, GS-teng was folded, twisted and stretched to 200% in sequence, which were all performed by hand for around 100 cyclic times respectively. Due to the flexibility and stretchability of basic GS-fiber as well as GS-teng, the GS-teng's appearance was recovered after deformation and the output voltage was not observed with obvious declining when it was compared with its initial value. The results indicated that the GS-teng was a robust energy generator device which could adapt to deformations like common textile. Moreover, the environment of human daily life has a wide temperature span from hot summer to cold winter. Consequently, as a power generating textiles, the GS-teng should also have steady output performance in such

temperature range. In this work, the friction silicone layer was commercial hollow fiber which had large working temperature range, and the concern of GS-teng's invalidation was thus focused on the inner gel electrode. Gel electrode was consisted of 3D frame network and swelling solvent, which could be easily embrittled by cold environment if the swelling solvent had higher freezing point such as water.[34] As exhibited in aforementioned paragraph, the swelling solvent of gel was PC which have a low freezing point of -49 ℃ and a high boiling point of 242 ℃. Accordingly, the prepared gel electrode had a wide working temperature range which could tolerate cold or hot environment in daily life. As shown in Fig 3b and SI video-1, the GS-teng was placed in a -20 ℃ fridge to demonstrate its resistance to cold environment and the output performance in such cold environment was tested by hand tapping. As expected, the embrittlement was not observed in GS-teng. The output voltage achieved 43 V which was slight inferior to its initial value in 25 ℃, as presented in Fig 3b. The slightly decrease was mainly due to the crimp of GS-teng, which was hard to fix in plate and further decreased the effective contact area with hand. Similarly, an oven with 45 ℃ was employed to test GS-teng's resistance to hot environment. The GS-teng's output voltage was maintained at 55 V which was similar with its output performance in 25 ℃. On the basis of these results, GS-teng exhibited excellent robustness to resist cold and hot environments in daily life, which was applicable and reliable in wide temperature span for energy harvesting.

Furthermore, the textile for human should be durable, which is also the requirement of TENG textile. Due to the contained swelling solvent in gel, gel based

electrode thus faced the challenge of dehydration along with time, which would undermine or even lose mechanical elasticity and conductivity of gel based electrode. In this work, the swelling solvent was selected as high boiling point solvent PC which was hard to be volatilized in daily life environment. Besides, the gel electrode was the inner core of GS-fiber which was encapsulated by outer silicone layer and further prevented the evaporation. That endowed the gel electrode with good anti-dehydration and the corresponding GS-teng's durability was also excellent. To demonstrate the GS-teng durability, the weight variation of GS-teng in 25 ℃ indoor environment and 45 ℃ environment were plotted in Fig S7. In 25℃ environment, GS-teng's weight showed very slight decrease after 30 days, which was a great improvement as compared to hydrogel electrode fiber (25% weight loss in 30 days).[48] Even in 45 ℃ environment, GS-teng's weight still maintained its 97% of initial weight after 30 days. The slight weight decrease illustrated the slight swelling solvent lose and good anti-dehydration of GS-teng. Accordingly, the triboelectric performance of GS-teng was kept because of gel electrode's good condition after 30 days. As shown in Fig S7b, the output voltages at different storing time were 44 V at 0 days, 44 V at 15 days and 42 V at 30 days in 25℃ environment, which was a steady value as compared to initial value. When GS-teng was stored in 45℃ environment for 30 days, the output voltage also exhibited steady value when it was compared to the initial output voltage. Consequently, the GS-teng was supposed to be a durable electricity generator textile and could bear high temperature environment for wearable device.

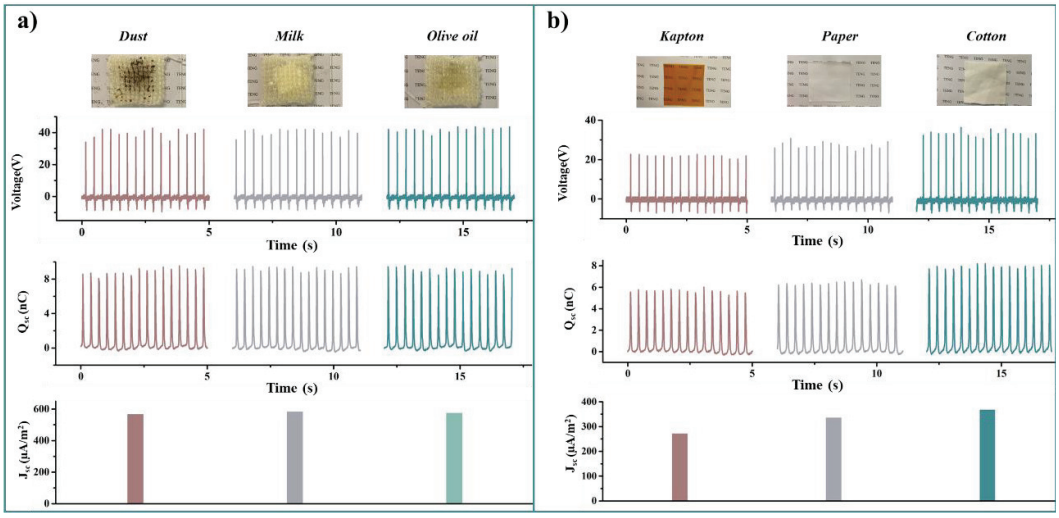

Figure 4. a) The output voltage, Q_{sc} and J_{sc} of GS-teng after it was washed from contaminant. b) The output voltage, Q_{sc} and J_{sc} of GS-teng with other paired friction materials.

Textile is exposed to multi-contaminants in daily life, which requires the textile's washability to remove contaminants and recover its function. Owing to the core/shell structure of GS-fiber, the outer friction layer of silicone was exposed to contaminants and the inner gel electrode was well protected by the outer silicone layer. The silicone layer had good stability and could facilely recover its friction function from contaminants via washing. As presented in Fig 4a, some common contaminants such as dust, milk and olive oil were poured on GS-teng to stain the textile for the purpose of washability exhibition. After water or detergent washing, the GS-teng was dried in the air and the appearance did not show obvious change. More importantly, the output performance also showed negligible change, indicating GS-teng was a washable textile for daily life. Furthermore, the scenario of daily life is various and the paired friction materials are not limited to triboelectrically positive nitrile glove. Other common triboelectrically positive materials such as Kapton, paper and cotton fabric were then employed to evaluate GS-teng's potential in electricity generator. Via periodical contact

and separation between such materials and GS-teng, output signal was thus generated. As shown in Fig 4b, an output signal of 36 V in output voltage, 8.2 nC in charge transfer, and 368 $\mu A/m^2$ in short-circuit current was observed when cotton was the paired material. When the GS-teng was paired with paper, the output performance was also excellent which was inferior to it of cotton. The output voltage, charge transfer and short-circuit current achieved 31 V, 6.7 nC and 272 $\mu A/m^2$, respectively. Cotton fabric and paper exhibited higher output performance than that of Kapton because the flexibility and softness would induce larger effective contact area, even Kapton had stronger electron losing ability. [49] The GS-teng's output performance in two-electrode working mode was further measured, which was presented in Fig S8. In general, the output performances in two-electrode working mode reached a higher level as compared to it in single-electrode working mode. Other paired materials for cloth were also tested to manifest the applicability of GS-teng. As shown in Fig S9, all of spandex, polyester and wool fabric could generate electric signals when force of 50 N with 3 Hz was applied to the TENG. On the basis of these results, GS-teng was believed to be a textile which could adapt to various types of triboelectrically positive materials in different daily life scenarios.

2.3 The output performance of GS-teng as a power source

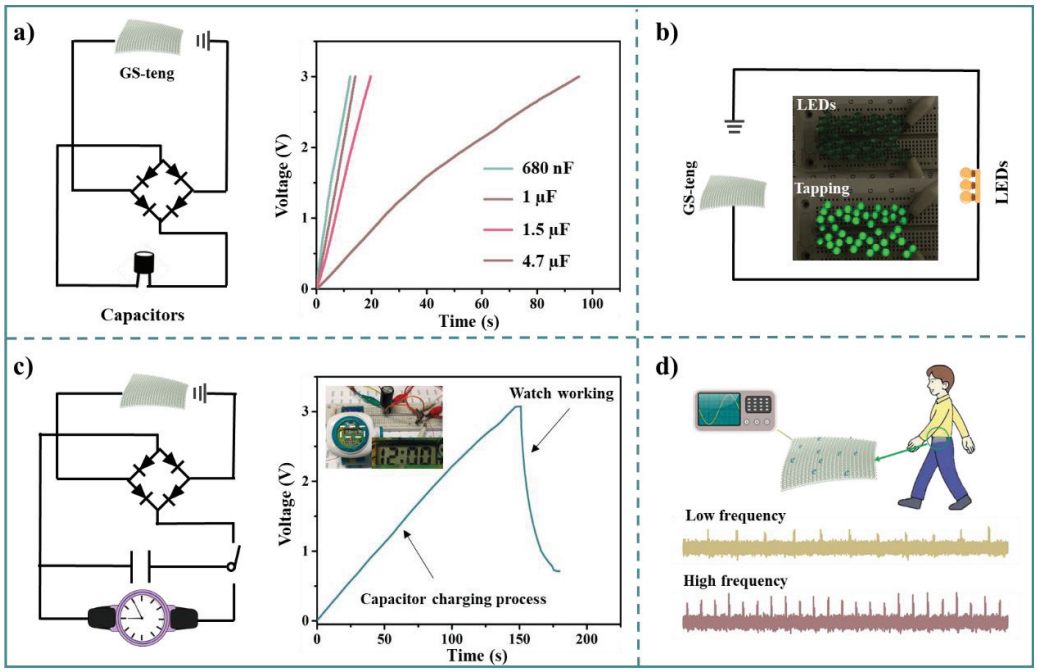

Figure 5. a) The circuit of capacitor charging and voltage curve of capacitor. b) The circuit of lighting 43 green LEDs and the corresponding photo. c) The circuit of driving electric watch and the corresponding voltage curve in charging and driving process. The inserted photo was the electric watch in working state. d) The GS-teng was applied for monitoring of arm swinging in walking.

GS-teng was subsequently connected to different external load to investigate its ability as a wearable power source and bio-mechanical energy harvesting device. As exhibited in Fig 5, when GS-teng was periodically tapped by hand in glove with a frequency of around 4 Hz, the electricity generated from the textile could be stored in capacitor, in which a rectifier was used to adjust the direction of GS-teng current. The capacitor charging curves were plotted in Fig 5a. The gradual increase of capacitors' voltage was observed in all capacitors' charging curves as the periodical hand tapping was performed on the GS-teng. The charging rates of different capacitors were 246 mV/s@680 nF, 213 mV/s@1.0 μF, 152 mV/s@1.5 μF and 32 mV/s@4.7 μF respectively when the capacitors' voltage was achieved at 3 V. The increasing capacitors' voltage illustrated that the electricity from the energy textile was

successfully stored. Moreover, GS-teng and 43 green LEDs were initially connected in a series circuit. The bio-mechanical energy from hand tapping was thus transferred into electricity by the GS-teng and the LEDs were consequently lightened with good brightness, as exhibited in SI video-2. Furthermore, as the electricity was stored by capacitor, the electricity was more concentrated and powerful which could drive many other electronics. For exhibition, a special circuit was designed, in which an additional circuit with an electric watch was connected in the original capacitor charging circuit through a hand switch, as exhibited in Fig 5c. As the capacitor's voltage reached to 3 V within 150 s, the circuit was changed by the switch to connect capacitor and the electric watch. Hence, the watch was successfully powered by the capacitor and the screen of watch illustrated that the watch was working. After 10 s, the capacitor's voltage decreased to around 1 V and the screen of watch stayed off as the consumption of electricity. All these results illustrated that the GS-teng was a successful wearable power source for energy harvesting.

The GS-teng also have the ability for monitoring arm swinging in walking for as a e-skin fabric, as shown in Fig 5d. The GS-teng was fixed on the hem of lab coat, which would be brought into periodical contact and separation with cuff in the process of the arm swinging. The output signal was consequently generated and observed, which monitored the arm swinging. The detection system was only based on GS-teng, on other part was introduced, implying that was a simple device with self-power source. Moreover, the signal frequency was increased with swinging frequency, which was sensitive to indicate walking frequency.

3. Conclusions

In summary, organogel electrode was proposed to construct triboelectric fiber (GS-fiber) and textile based TENG. GS-fiber was prepared from photo-crosslinking of organogel in continuous transparent silicone hollow fiber, in which silicone hollow fiber was not only the mold for the gel electrode fiber but also the outer friction layer of GS-fiber. The triboelectric fiber was in an organogel/silicone core/shell structure, in which shell silicone layer was the friction materials and organogel was the back electrode. The soft and stretchable core gel electrode endowed GS-fiber with good stretchability and avoided cracking problem of metallic wire based triboelectric fiber. In addition, the solid form of gel also avoided leakage problem of liquid conductor and the GS-fiber thus could be tailored in designed size for textiles. More importantly, GS-fiber has the potentials of large-scale production because of the simple preparation process and 30 meter GS-fiber was prepared in this work. The GS-fiber was subsequently applied to knit textile based TENG, GS-teng. The GS-teng was wearable device and could harvest the bio-mechanical energy to drive electronics, demonstrating promising potential in wearable electronics, e-skin, etc. This work demonstrated that organogel electrode has great potential in triboelectric fiber, which makes a remarkable progress towards the target of industry application in textile based TENG.

4. Experiment section

Materials and Characterization

Lithium bis(trifluoromethylsulfonyl)imide (LiTFSI) was the product of Shanghai Aladdin Bio-Chem Technology Co., LTD and Propylene carbonate (PC) was obtained from Alfa Aesar. The silicone hollow fiber was supplied by Shanghai Hongtu Rubber Plastic Product Co.,Ltd, which was 1 mm in outer diameter and 0.5 mm in inner diameter. 4-acryloylmorpholine (ACMO, monomer), N,N'-Methylenebisacrylamide (MBA, cross-linker) and 1-hydroxycyclohexyl phenyl ketone (photoinitiator 184) were purchased from Dieckmann company. All reagents were used as received without further purification.

PerkinElmer. Inc, Spectrum100 was applied to FTIR test of gel. Button/key durability life test machine, ZX-A03, Zhongxingda Shenzhen provided periodically external force to test the TENG textile's triboelectric performance. The applied force was 50 N and the spacer distance was 1 cm unless otherwise specified. Four-probe tester STST-2258A, Suzhou Jingge Electronic Co. LTD was the equipment for resistivity of gel electrode test. The capacitors were electrolytic capacitors of CHANGX brand, which were bought from Dongguan Chengxing Electronic Co., Ltd. Instron5900 was employed to uniaxial tensile test. Oscilloscope was applied to record output voltage, which was a Keysight Infiniivision DSOX3024T. The output current and transfer charge was recorded by Keithley 6514 system electrometer of Tektronix, Inc.

Preparation of organogel electrode PACMO-LiTFSI, triboelectric GS-fiber and textile GS-teng

The fiber shape gel electrode PACMO-LiTFSI was synthetized by the photo-crosslinking of ACMO in PC solution.[33, 50] LiTFSI was first dissolved in PC to prepare 0.5 M solution. Subsequently, ACMO monomer and LiTFSI's PC solution were mixed at the volume ratio of 50:50. Finally, MBA and photoinitiator 184 were added to the mixed solution and the molar ratio was cross-linker 0.1% and initiator 1% of monomer respectively, which was pre-cured solution for gel electrode.

The pre-cured solution was then pumped into silicone hollow fiber with a syringe transfer. The length of silicone hollow fiber was decided by demand and the length in this work was 30 m for the demonstration of large-scale production. After that, silicone hollow fiber with pre-cured solution was put into a 365 nm ultraviolet light box of 75 W and irradiated for 40 mins to cure the solution. The fiber shape PACMO-LiTFSI gel electrode and triboelectric GS-fiber were consequently obtained.

The GS-fiber was utilized to prepare TENG textile. As the solid state of gel electrode, the GS-fiber could be tailored in designed length like traditional fiber. 3 m GS-fiber was tailored in this work to prepare 5×5 cm^2 textile GS-teng by hand knitting.

Washability of GS-teng

Dust was poured on GS-teng to stain the textile. The dust was then removed by water washing. After that, the GS-teng was dried in the air at room temperature. The output performance was tested when the residual water on the surface of GS-teng was volatilized. The applied force was same with output performance test's applied force. After the dust washing test, milk and olive oil were also tested in similar way. Detergent was employed to remove olive oil as it hard to be cleaned by water.

Acknowledgements

The authors would like to acknowledge the funding support from the Research Grants Council of the Hong Kong Special Administrative Region, China (Project No. PolyU 15209020) and the Hong Kong Polytechnic University (Project No. G-YZ4H and G-YWA2) for the work reported here.

References:

[1] P. Zhang, Y. Chen, Z.H. Guo, W. Guo, X. Pu, Z.L. Wang, Advanced Functional Materials, 30 (2020).
[2] J. Wang, S. Li, F. Yi, Y. Zi, J. Lin, X. Wang, Y. Xu, Z.L. Wang, Nat Commun, 7 (2016) 12744.
[3] Z.M. Lin, J. Yang, X.S. Li, Y.F. Wu, W. Wei, J. Liu, J. Chen, J. Yang, Advanced Functional Materials, 28 (2018).
[4] Q. Shi, T. He, C. Lee, Nano Energy, 57 (2019) 851-871.
[5] J. Liu, X.Y. Daphne Ma, Z. Wang, L. Xu, T. Xu, C. He, F. Wang, X. Lu, ACS Appl Mater Interfaces, 12 (2020) 7442-7450.
[6] X. Cao, Y. Jie, N. Wang, Z.L. Wang, Advanced Energy Materials, 6 (2016).
[7] Z.L. Wang, T. Jiang, L. Xu, Nano Energy, 39 (2017) 9-23.
[8] X. Guan, B. Xu, J. Gong, Nano Energy, 70 (2020).
[9] K. Dong, Y.C. Wang, J. Deng, Y. Dai, S.L. Zhang, H. Zou, B. Gu, B. Sun, Z.L. Wang, ACS Nano, 11 (2017) 9490-9499.
[10] K. Dong, J. Deng, Y. Zi, Y.C. Wang, C. Xu, H. Zou, W. Ding, Y. Dai, B. Gu, B. Sun, Z.L. Wang, Adv Mater, 29 (2017).
[11] F.R. Fan, W. Tang, Z.L. Wang, Adv Mater, 28 (2016) 4283-4305.
[12] G.R. Zhao, Y.W. Zhang, N. Shi, Z.R. Liu, X.D. Zhang, M.Q. Wu, C.F. Pan, H.L. Liu, L.L. Li, Z.L. Wang, Nano Energy, 59 (2019) 302-310.
[13] X. Chen, Y. Wu, J. Shao, T. Jiang, A. Yu, L. Xu, Z.L. Wang, Small, 13 (2017).
[14] F.R. Fan, Z.Q. Tian, Z.L. Wang, Nano Energy, 1 (2012) 328-334.
[15] J. Liu, L. Gu, N. Cui, Q. Xu, Y. Qin, R. Yang, Research (Wash D C), 2019 (2019) 1091632.
[16] Z.L. Li, M.M. Zhu, Q. Qiu, J.Y. Yu, B. Ding, Nano Energy, 53 (2018) 726-733.
[17] W. Gong, C. Hou, J. Zhou, Y. Guo, W. Zhang, Y. Li, Q. Zhang, H. Wang, Nat Commun, 10 (2019) 868.
[18] C.S. Wu, A.C. Wang, W.B. Ding, H.Y. Guo, Z.L. Wang, Advanced Energy Materials, 9 (2019).

[19] J.L. Gong, B.G. Xu, X.Y. Guan, Y.J. Chen, S.Y. Li, J. Feng, Nano Energy, 58 (2019) 365-374.
[20] T.T. Jing, B.G. Xu, Y.J. Yang, Nano Energy, 74 (2020).
[21] K. Dong, X. Peng, J. An, A.C. Wang, J. Luo, B. Sun, J. Wang, Z.L. Wang, Nat Commun, 11 (2020) 2868.
[22] W. Paosangthong, R. Torah, S. Beeby, Nano Energy, 55 (2019) 401-423.
[23] J. Shi, S. Liu, L. Zhang, B. Yang, L. Shu, Y. Yang, M. Ren, Y. Wang, J. Chen, W. Chen, Y. Chai, X. Tao, Adv Mater, 32 (2020) e1901958.
[24] K. Dong, X. Peng, Z.L. Wang, Adv Mater, 32 (2020) e1902549.
[25] C. Dong, A. Leber, T. Das Gupta, R. Chandran, M. Volpi, Y. Qu, T. Nguyen-Dang, N. Bartolomei, W. Yan, F. Sorin, Nat Commun, 11 (2020) 3537.
[26] Y. Yang, N. Sun, Z. Wen, P. Cheng, H. Zheng, H. Shao, Y. Xia, C. Chen, H. Lan, X. Xie, C. Zhou, J. Zhong, X. Sun, S.T. Lee, ACS Nano, 12 (2018) 2027-2034.
[27] W. Wang, A.F. Yu, X. Liu, Y.D. Liu, Y. Zhang, Y.X. Zhu, Y. Lei, M.M. Jia, J.Y. Zhai, Z.L. Wang, Nano Energy, 71 (2020).
[28] X.F. Wang, Y.J. Yin, F. Yi, K.R. Dai, S.M. Niu, Y.Z. Han, Y. Zhang, Z. You, Nano Energy, 39 (2017) 429-436.
[29] X. He, Y.L. Zi, H.Y. Guo, H.W. Zheng, Y. Xi, C.S. Wu, J. Wang, W. Zhang, C.H. Lu, Z.L. Wang, Advanced Functional Materials, 27 (2017).
[30] C. Lee, S. Yang, D. Choi, W. Kim, J. Kim, J. Hong, Nano Energy, 57 (2019) 353-362.
[31] X. Pu, L. Li, M. Liu, C. Jiang, C. Du, Z. Zhao, W. Hu, Z.L. Wang, Adv Mater, 28 (2016) 98-105.
[32] Z.M. Tian, J. He, X. Chen, Z.X. Zhang, T. Wen, C. Zhai, J.Q. Han, J.L. Mu, X.J. Hou, X.J. Chou, C.Y. Xue, Nano Energy, 39 (2017) 562-570.
[33] Y.Y. Gao, L. Shi, S.Y. Lu, T.X. Zhu, X.Y. Da, Y.H. Li, H.T. Bu, G.X. Gao, S.J. Ding, Chemistry of Materials, 31 (2019) 3257-3264.
[34] L.J. Sun, S. Chen, Y.F. Guo, J.C. Song, L.Z. Zhang, L.J. Xiao, Q.B. Guan, Z.W. You, Nano Energy, 63 (2019).
[35] X.F. Pan, Q.H. Wang, R.S. Guo, Y.H. Ni, K. Liu, X.H. Ouyang, L.H. Chen, L.L. Huang, S.L. Cao, M.Y. Xie, Journal of Materials Chemistry A, 7 (2019) 4525-4535.
[36] A.V. Salvekar, W.M. Huang, R. Xiao, Y.S. Wong, S.S. Venkatraman, K.H. Tay, Z.X. Shen, Acc Chem Res, 50 (2017) 141-150.
[37] P. Li, Z. Jin, L. Peng, F. Zhao, D. Xiao, Y. Jin, G. Yu, Adv Mater, 30 (2018) e1800124.
[38] S.K. Nalluri, N. Shivarova, A.L. Kanibolotsky, M. Zelzer, S. Gupta, P.W. Frederix, P.J. Skabara, H. Gleskova, R.V. Ulijn, Langmuir, 30 (2014) 12429-12437.
[39] Y. Jian, B. Wu, X. Le, Y. Liang, Y. Zhang, D. Zhang, L. Zhang, W. Lu, J. Zhang, T. Chen, Research (Wash D C), 2019 (2019) 2384347.
[40] X. Pu, M. Liu, X. Chen, J. Sun, C. Du, Y. Zhang, J. Zhai, W. Hu, Z.L. Wang, Sci Adv, 3 (2017) e1700015.
[41] K. Parida, V. Kumar, W. Jiangxin, V. Bhavanasi, R. Bendi, P.S. Lee, Adv Mater, 29 (2017).

[42] T. Liu, M. Liu, S. Dou, J. Sun, Z. Cong, C. Jiang, C. Du, X. Pu, W. Hu, Z.L. Wang, ACS Nano, 12 (2018) 2818-2826.
[43] P. Lv, L. Shi, C. Fan, Y. Gao, A. Yang, X. Wang, S. Ding, M. Rong, ACS Appl Mater Interfaces, 12 (2020) 15012-15022.
[44] S. Naficy, T.Y.L. Le, F. Oveissi, A. Lee, J.C. Hung, S.G. Wise, D.S. Winlaw, F. Dehghani, Advanced Materials Interfaces, 7 (2019).
[45] T. Jing, B. Xu, Y. Yang, M. Li, Y. Gao, Nano Energy, 78 (2020).
[46] J. Song, S. Chen, L. Sun, Y. Guo, L. Zhang, S. Wang, H. Xuan, Q. Guan, Z. You, Adv Mater, 32 (2020) e1906994.
[47] J. Wu, Z. Wu, H. Xu, Q. Wu, C. Liu, B.-R. Yang, X. Gui, X. Xie, K. Tao, Y. Shen, J. Miao, L.K. Norford, Materials Horizons, 6 (2019) 595-603.
[48] L. Shuai, Z.H. Guo, P. Zhang, J. Wan, X. Pu, Z.L. Wang, Nano Energy, 78 (2020).
[49] H. Zou, Y. Zhang, L. Guo, P. Wang, X. He, G. Dai, H. Zheng, C. Chen, A.C. Wang, C. Xu, Z.L. Wang, Nat Commun, 10 (2019) 1427.
[50] L. Shi, R.S. Yang, S.Y. Lu, K. Jia, C.H. Xiao, T.Q. Lu, T.J. Wang, W. Wei, H. Tan, S.J. Ding, Npg Asia Materials, 10 (2018) 821-826.